Modeling Chromatographic Chiral Separations under Nonlinear Competitive Conditions

Cristiano Migliorini and Marco Mazzotti
ETH Zürich, Institut für Verfahrenstechnik, CH-8092 Zürich, Switzerland

Gianmarco Zenoni, MariaPia Pedeferri, and Massimo Morbidelli
ETH Zürich, Laboratorium für Technische Chemie, CH-8092 Zürich, Switzerland

The chromatographic separation of Tröger's base enantiomers with ethanol as eluent on microcrystalline triacetate cellulose (CTA) was studied. Binary competitive adsorption equilibrium data measured were interpreted using ideal adsorbed solution and real adsorbed solution (RAS) theory. Both models were used to simulate a set of column breakthrough experiments. The competitive behavior of the two enantiomers is quantitatively discussed and the reliability of the two models is assessed. The results show that the RAS model can describe with good accuracy the complex competitive adsorption behavior exhibited by the CTA/Tröger's base model system. This conclusion is expected to apply to the adsorption of the other enantiomeric mixtures on chiral stationary phases.

Introduction

The optimization of enantiomer separations at the preparative scale and the scale-up of separation processes from batch chromatography to continuous simulated moving-bed separations requires a proper understanding of the adsorption equilibria under nonlinear conditions. Under analytical conditions only the thermodynamic properties at infinite dilution are determined, while the separation processes just mentioned are operated in the nonlinear region. So far, in most cases the equilibria of enantiomers on chiral stationary phases have been described with empirical models based on the multicomponent Langmuir (Küsters et al., 1995), modified Langmuir (Nicoud et al., 1993; Heuer et al., 1998), and bi-Langmuir isotherms (Jacobson et al., 1990; Fornstedt et al., 1997; Pais et al., 1997). A valuable alternative to the quantitative description of the competitive adsorption is given by rigorous thermodynamic models such as the ideal adsorbed solution (IAS) or the real adsorbed solution (RAS) model. The objective of this work is to extend the use of these models to chiral-selective adsorption and to assess their ability to achieve the desired accuracy in the description of competitive experimental data. The separation of the Tröger's base enantiomers on crystalline triacetate cellulose (CTA) will be used as a model system.

CTA is a cheap chiral stationary phase that has good mechanical properties and can resolve many racemic mixtures with good selectivity (Francotte et al., 1985). Unfortunately, the efficiency of this stationary phase is rather low (Rizzi, 1989a; Jacobson et al., 1993; Seidel-Morgenstern and Guiochon, 1993). Therefore the performance of CTA is the result of a trade-off between a good selectivity and a low efficiency, as in the case of the Tröger's base enantiomers, where it exhibits a selectivity value of about 2 (Rizzi, 1989a; Seidel-Morgenstern and Guiochon, 1993; Pedeferri et al., 1999). Under these conditions large peak broadenings are often obtained, that limit the use of this material to analytical purposes (Rizzi, 1989a). Also the scale-up of separations on CTA is not straightforward, although it is expected that this stationary phase exhibits a good potential in chiral SMB separations since their performances are not strongly affected by a low column efficiency (Migliorini et al., 1999). This is confirmed by the high purity values, of 98%, obtained by Pedeferri et al. (1999).

It is worth noting that with respect to other stationary phases, CTA shows a relatively high loading capacity that is best exploited by separation processes operating close to saturation conditions (Rizzi, 1989b). This is the case of SMB continuous separations, because of a higher productivity (Francotte and Richert, 1997) and a lower sensitivity to column efficiency (Migliorini et al., 1998).

The adsorption of the Tröger's base enantiomers, (±)-TB, on CTA has been previously investigated and it has been shown that the two enantiomers show a different adsorption

Correspondence concerning this article should be addressed to M. Morbidelli.

equilibrium behavior (Seidel-Morgenstern et al., 1993). The adsorption of the (−)-TB enantiomer can be described with a Langmuir isotherm, while the (+)-TB enantiomer shows an unfavorable adsorption behavior at low concentration that becomes favorable at high concentrations. This leads to the unusual increase (followed by a decrease) of the retention time of a pulse of the more retained enantiomer when larger volumes of analyte are injected (Seidel-Morgenstern et al., 1993; Seidel-Morgenstern and Guiochon, 1993). Other interesting aspects of the adsorption behavior of this system have been evidenced, such as a strong dependence of the efficiency on the flowrate, the temperature, and the solvent composition (Rizzi, 1989a,b; Jacobson et al., 1993; Rearden et al., 1998). On the other hand, not much attention has been paid to the binary competitive adsorption behavior, which has been estimated with the IAS model but without experimental verification (Seidel-Morgenstern and Guiochon, 1993). The measurement of the multicomponent competitive adsorption behavior is in fact complicated by the need to determine the absolute amount of each enantiomer adsorbed on the stationary phase. In this work this is made possible by a suitable detection scheme that allows a rather detailed analysis of the thermodynamics of adsorption, based on accurate measurements of the band profiles of each enantiomer in frontal runs.

In the following, the experimental technique is first briefly summarized. Then the IAS and RAS models are introduced and the consequences of their application to our model system are discussed. The two models are compared with the experimental results to assess their reliability. This analysis allows the the proper understanding of the column breakthrough experiments that are discussed in the central part of this article after the introduction of the column model. Finally, pulse experiments are reported and discussed.

Experimental Setup

Columns and chemicals

Unsupported microcrystalline cellulose triacetate beads in the 15−25-μm range (Merck 16362) were packed in the stainless-steel chromatographic column (0.46 cm ID × 25 cm). The stationary phase has been boiled in pure ethanol for 30 min to let it swell. The suspension was packed at room temperature under 200-bar pressure, with ethanol as a pushing solvent at a flow rate of 4 cm^3/min. The column contained 3.9 g of swollen stationary phase; the mass of stationary phase is measured by weighting the column before and after packing and subtracting the mass of solvent in all voids. The pure (−)-TB and (+)-TB enantiomers have been purchased from Aldrich; all binary mixtures have been prepared by properly mixing the pure enantiomers. Pure ethanol used as the mobile phase, as well as 1,3,5-tri-tert-butylbenzene (TTBB) used to measure the column porosity, have been purchased from Fluka. All chemicals were used as received.

Analytical methods

The flow rate is delivered by an HPLC pump (Jasco PU 987) and kept constant at the value of 0.5 cm^3/min. The analysis is performed under isocratic conditions on an HP 1090 liquid cromatograph equipped with a binary system pump, autosampler, and a thermostatted column compartment kept at 323 K. The chromatograph is connected in series with a UV detector (Jasco UV-970, wavelength 283 nm) and a polarimeter (Jasco OR-990). The data are collected through a computer data-acquisition system and elaborated using a Labview program. The response of the UV detector is proportional to the sum of the concentrations of the two enantiomers, while the signal of the polarimeter is proportional to their difference. After calibration of the detectors and careful measurement of the dead volumes between the two analytical cells (needed to synchronize the two signals), it is possible to measure on-line the concentration of each enantiomer. The detectors are located in a box where the temperature is kept at the value of 296 K $\pm$ 0.2; this is guaranteed by a suitable control loop that acts on a heat exchanger through which cooling air is circulated. Without this layout the temperature in the surroundings of the detectors would increase considerably above the value during calibration, due to heat dissipation of the detector lamps. A detailed description of the setup for on-line enantiomer concentration monitoring is reported by Zenoni et al. (1999).

Adsorption Equilibria

Single-component isotherms

An overall void fraction of the column $\epsilon = 0.59$ was determined by injecting TTBB pulses (Rearden et al., 1998). Although TTBB is slightly retained on CTA (Jacobson et al., 1993), this substance was used in the determination of column porosity in most earlier studies (Seidel-Morgenstern and Guiochon, 1993; Rearden et al., 1998; Pedeferri et al., 1999). It is known that the results of the porosity measurement depend on the type of molecule used, on its hydrophobicity and eluent composition, so that an absolute particle and overall porosity cannot be given (Rizzi, 1989a). However, the small value of the retention factor of TTBB and its small change with temperature suggests that the error in the measurement of the column porosity is rather small.

The adsorption isotherms of the pure enantiomers were determined through frontal analysis experiments, as described in detail elsewhere (Pedeferri et al., 1999). Note that since the column efficiency is rather low, the frontal analysis technique is the most reliable method for determining the adsorption isotherms (Seidel-Morgenstern et al., 1993). For the same reason that area measurement was preferred instead of the half-height method (Rearden et al., 1998). The adsorption of the less retained enantiomer (−)-TB can be described with a Langmuir isotherm:

$$n_B^{\circ} = \frac{2.18 c_B}{1 + 0.065 c_B}, \tag{1}$$

where c is the fluid-phase concentration is grams per liter of solution, n is the corresponding adsorbed amount in grams per liter of swollen stationary phase, and the subscript B refers to the less retained enantiomer.

On the other hand, the isotherm of the more retained enantiomer (+)-TB exhibits an inflection point, and has been described with an empirical isotherm (the so-called quadratic

isotherm):

$$n_A^\circ = \frac{6.986 c_A (0.627 + 0.594 c_A)}{1 + 0.627 c_A + 0.297 c_A^2}. \qquad (2)$$

The different behavior of the two enantiomers is evidenced by plotting the equilibrium data in the n/c vs. n diagram. In this plane the Langmuir isotherm is represented by a straight line while the quadratic isotherm shows a maximum, corresponding to the inflection point in the isotherm, at a concentration of about 0.28 g/L. The loading capacities of the two enantiomers are also remarkably different, the (−)-TB exhibiting the larger one (Seidel-Morgenstern and Guiochon, 1993; Pedeferri et al., 1999).

IAS and RAS models of binary adsorption

In the following the competitive binary adsorption of the Tröger's base enantiomers from a dilute solution in ethanol is studied. This is a rather typical situation in chiral chromatography, where on the one hand, the solubility of the chiral molecules is low, hence the concentration in the solution is small, while on the other hand, the loadability of the chiral stationary phase (CSP) is also small, hence even at low fluid-phase concentration competitive nonlinear adsorption occurs. For the description of this phenomenon we adopt the rigorous thermodynamic framework given by the IAS and the RAS theory.

The IAS model establishes a method for predicting multisolute adsorption using only data for single solute adsorption (Myers and Prausnitz, 1965). This method was first proposed for adsorption of gas mixtures, and then extended to multisolute adsorption from dilute liquid solutions (Radke and Prausnitz, 1972). The IAS model reduces to the well-known multicomponent competitive Langmuir isotherm if each single-component isotherm is a Langmuir with the same saturation capacity; this is rarely the case for enantiomers (Golshan-Shirazi and Guiochon, 1991). When the solute loading is large, the simplifying assumptions of the IAS theory must be relaxed in order to account for solute–solute interactions in the adsorbed phase. Thus the IAS model can be replaced by the RAS model where the deviations from the ideality of the adsorbed phase are lumped into an activity coefficient (Radke and Prausnitz, 1972; Myers, 1986; Paludetto et al., 1987; Talu and Myers, 1988; Gamba et al., 1989). It is worth noting that the deviations from the ideal behavior calculated with the RAS model might be due to surface heterogeneity rather than to nonideal interaction between the adsorbed molecules (Myers, 1983). Since the adsorption sites on CSPs are often classified as chiral selective and nonselective (Jacobson et al., 1990), it would be reasonable to describe the surface as a collection of sites of different adsorption characteristics as it is done, for example, by the heterogeneous IAS model (Valenzuela et al., 1988). However, in order to keep the number of adjustable parameters low, in this work we will introduce only activity coefficients and no surface heterogeneity. The objective is a model that quantitatively describes nonlinear binary adsorption, more than its physical interpretation.

In many practical cases, for example, in the pharmaceutical industry, the solubility of complex enantiomeric molecules is rather small (a few grams per liter), and therefore the assumption of dilute solutions is realistic and general. In this case, the equality of the chemical potentials for solute i can be expressed at constant temperature in the form (Radke and Prausnitz, 1972):

$$c_{\text{tot}}\, y_i = c_i = \gamma_i c_i^\circ(\psi)\, z_i \qquad i = A,\ B, \qquad (3)$$

where the activity coefficient in the adsorbed phase $\gamma_i = \gamma_i(\psi, \mathbf{z})$ is a function of the adsorbed phase composition $\mathbf{z}$ and the reduced spreading pressure ψ. The single-component concentration c_i^0 in equilibrium at the same spreading pressure and temperature as the mixture, is given by the Gibbs isotherm,

$$\psi = \frac{A\Pi}{RT} = \int_0^{c_i^\circ} \frac{n_i^\circ(c)}{c}\, dc \qquad i = A,\ B, \qquad (4)$$

where $n_i^\circ(c)$ indicates the single-component equilibrium isotherm. These equations can be used together with the stoichiometric relationship in the adsorbed phase:

$$\sum_{i = A,\ B} z_i = 1 \qquad (5)$$

to calculate, for a given liquid phase composition c, the adsorbed phase composition $\mathbf{z}$ and the reduced spreading pressure ψ.

The IAS model assumes an ideal behavior of the adsorbed phase, that is, $\gamma_i = 1$. Therefore the calculations with this model require only the knowledge of the single-component isotherms. On the other hand, the RAS model needs binary data to estimate the adjustable binary interaction parameters to be used in a suitable model for the activity coefficients. In this work, the Wilson model for liquid mixtures has been used, including the empirical spreading-pressure dependence, as suggested by Myers (Myers, 1986; Talu and Zwiebel, 1986). Thus, the activity coefficient is given by

$$\ln \gamma_i = (1 - e^{-\alpha\psi}) \left[1 - \ln \left(\sum_{j = A,\ B} z_j \Lambda_{i,j} \right) - \sum_{k = A,\ B} \left(\frac{z_k \Lambda_{k,i}}{\sum_{j = A,\ B} z_j \Lambda_{k,j}} \right) \right] \qquad \Lambda_{i,i} = 1 \qquad i = A,\ B. \qquad (6)$$

It is worth noting that the preceding expression for the activity coefficient given by Eq. 6 is thermodynamically consistent (Talu and Zwiebel, 1986), while others that do not include the spreading-pressure dependence are not (Radke and Prausnitz, 1972; Costa et al., 1981; Gamba et al., 1990), since they do not satisfy the condition $\gamma_i \to 1$ as $\Pi \to 0$, that is, at zero surface coverage. In general, the change of the spreading pressure with composition is small when compared with the strong effect of the total pressure or the total concentration for adsorption from gas and dilute liquid mixtures, respectively. Therefore the preceding models gave good results in interpreting sets of experimental data involving limited

changes in the spreading pressure. As shown in the sequel, however, the system studied here exhibits a strong dependence of the spreading pressure on the composition, and therefore a complete thermodynamic model is required not only to enforce the correct limit at infinite dilution, but also to describe accurately the binary data at high concentrations.

Note that the RAS model given earlier involves three adjustable parameters of the model (Λ_{AB}, Λ_{BA}, α), providing the flexibility necessary to describe very complex adsorbed-phase behaviors (Myers, 1986; Talu and Zwiebel, 1986), such as in the case of enantiomers on chiral stationary phases. The total amount adsorbed is calculated from

$$\frac{1}{n_{\text{tot}}} = \sum_{i=A,B} \frac{z_i}{n_i^{\circ}(c_i^{\circ})} + \sum_{i=A,B} z_i \left(\frac{\partial \ln \gamma_i}{\partial \psi} \right)_{T,z} \qquad (7)$$

where the second term in the righthand side accounts for the molar area change upon mixing (Myers and Prausnitz, 1965). Finally, the adsorbed phase composition for each compound is given by

$$n_i = n_{\text{tot}} z_i \qquad i = A, B. \qquad (8)$$

It is worth noting that when simulating the dynamics of a chromatographic column we need a fast and reliable numerical procedure to calculate the adsorbed amount of each species on the stationary phase at equilibrium. The IAS and RAS models are considered demanding from the numerical and computational point of view (Seidel-Morgenstern and Guiochon, 1993). Approximate solutions (LeVan and Vermeulen, 1981) and suggestions for a fast implementation of these models (O'Brien and Myers, 1985) are available in the literature. In our example since the integrals in Eq. 4 are explicit, the implementation of the numerical procedure is largely simplified. This allows the coding of a very effective algorithm for the solution of the system of Eqs. 3 to 5, which eventually results in a computational time of a few minutes on a PC (Pentium II 266 MHz) for each of the column breakthrough simulations reported in the following.

Comparison with binary experimental data

The frontal-analysis technique used to determine the single-component isotherms (Pedeferri et al., 1999) also can be used to determine binary adsorption equilibrium data. Since the developed on-line analytical method allows the concentration profile of each enantiomer to be measured separately. From this, it is possible to calculate the amount of each enantiomer adsorbed at equilibrium. In principle, one adsorption experiment is sufficient to determine the adsorbed phase concentration of the two enantiomers. In this work, however, each adsorption experiment has been followed by complete desorption, until the column was equilibrated with pure solvent. This allows the mass balances for each point to be double-checked. The data measured with frontal analysis using binary mixtures with various concentrations are reported in Table 1, in terms of the experimental values of the adsorbed phase concentration of each enantiomer at equilibrium. The data are divided into four series, each corresponding to a different relative composition of the binary mixture (that is, $c_A/c_B = 25/75$, 60/40, 50/50, and 60/40), with increasing values of liquid-phase total concentration. In the table the relative errors, that is $(n_i^{\text{mod}} - n_i^{\text{exp}})/n_i^{\text{exp}}$, calculated with the IAS and RAS models, are reported. The parameters of the RAS model have been determined by fitting the data reported in Table 1, with the objective of minimizing the square relative error over the whole set of points. The fitting yields $\Lambda_{AB} = 0.57$, $\Lambda_{BA} = 1.24$, and $\alpha = 0.42$.

Some peculiarities in the behavior of the system under examination can be evidenced by looking at the model results. In particular it is found that the system exhibits positive devi-

Table 1. Amount Each Enantiomer Adsorbed on the Stationary Phase (as g of pure enantiomer per L of swollen CTA) at Different Relative Compositions of the Mobile Phase in the Series of: 25/75, 40/60, 50/50, 60/40

	Mobile Phase			Stationary Phase		IAS Relative Error		RAS Relative Error	
Run	c_A/c_B	c_A (g/L)	c_B (g/L)	n_A (g/L)	n_B (g/L)	A	B	A	B
A	25/75	0.113	0.329	0.507	0.709	+0.6	−0.8	−4.4	−5.1
B	25/75	0.226	0.658	0.987	1.348	+3.3	+1.1	−3.5	−4.7
C	40/60	0.516	0.779	2.234	1.466	+2.3	+5.3	−1.2	−4.2
D	40/60	1.032	1.558	3.920	2.630	+2.9	+2.3	+1.2	−7.4
E	50/50	0.106	0.104	0.467	0.229	+0.4	+0.7	−1.2	−3.6
F	50/50	0.209	0.213	0.957	0.433	−0.2	+5.5	−2.7	−1.4
G	50/50	0.315	0.318	1.443	0.626	−0.0	+7.0	−2.7	−1.8
H	50/50	0.421	0.423	1.911	0.806	+0.3	+8.1	−2.3	−1.8
I	50/50	0.531	0.532	2.380	0.969	+0.4	+10.1	−2.1	−0.5
J	50/50	0.782	0.804	3.382	1.309	−0.6	+14.5	−2.4	+3.8
K	50/50	1.067	1.095	4.344	1.672	−1.1	+14.0	−2.1	+3.1
L	50/50	1.575	1.608	5.703	2.186	−2.5	+13.6	−2.3	+2.9
M	60/40	0.308	0.209	1.149	0.388	−2.3	+13.2	−4.2	+4.8
N	60/40	0.616	0.418	2.870	0.715	−3.5	+15.4	−5.1	+4.0
O	60/40	0.923	0.626	4.094	0.997	−3.9	+15.7	−4.8	+3.2
P	60/40	1.231	0.835	5.131	1.253	−4.4	+14.7	−4.6	+1.8
Q	60/40	1.539	1.044	6.019	1.505	−5.4	+12.2	−5.1	−1.1

Note: The relative error of the IAS and RAS models is defined as the difference between the prediction of the model and the experimental measure divided by the experimental value, that is, $(n_i^{mod} - n_i^{\text{exp}})/n_i^{\text{exp}}$.

ations from Raoult's law. As shown in Figure 1 increasing selectivity values are found at constant total concentration c_{tot} as the mol fraction of the more retained enantiomer A increases, while the opposite behavior is usually found experimentally in the case of adsorption on heterogeneous surfaces (Myers, 1983). This can be explained by considering the following expression for selectivity derived from Eq. 3:

$$S_{A,B} = \frac{z_A/y_A}{z_B/y_B} = \frac{\overset{\circ}{c}_B \gamma_B}{\overset{\circ}{c}_A \gamma_A}. \tag{9}$$

It can be seen that when the liquid-phase composition changes at constant total concentration, the ratio $\overset{\circ}{c}_B/\overset{\circ}{c}_A$ remains nearly constant, while the spreading pressure changes. Hence the behavior of the selectivity can be explained considering only the positive deviation of the activity coefficient from Raoult's law as follows: as y_A increases toward one, $\gamma_A \to 1$ and $\gamma_B \to \gamma_B^{\infty} > 1$, thus causing the selectivity (Eq. 9) to increase. Therefore, the positive deviation from Raoult's law is related to the selectivity increase at increasing molar fraction of the stronger component, and there is no consistency with the typical consequences of adsorption heterogeneity as described by Myers (Myers, 1983). This anomalous behavior has probably to be attributed to the rather peculiar interaction between enantiomers and chiral phases, which certainly differ from those encountered in usual heterogeneous adsorption systems.

The application of the IAS and RAS model to systems where at least one single-component isotherm is not a Langmuir may have consequences that deserve to be mentioned. Let us consider in the n/c vs. n-plane parametric curves at constant concentration of the other enantiomer calculated using the IAS model, as shown in Figure 2. The broken curve corresponds to the single-component isotherm of the (+)-TB enantiomer, that is, $c_B = 0$, while the solid curves have been obtained with increasing concentration of the (−)-TB enantiomer.

It can be seen that the curves at the left side of the graph exhibit a crossover. This corresponds to the fact that the Henry constant of (+)-TB enantiomer goes through a maximum, as predicted by the IAS model as the concentration of (−)-TB enantiomer increases. In addition, the maximum in the single-component isotherm of the (+)-TB enantiomer becomes less pronounced and eventually vanishes as the concentrations of the (−)-TB enantiomer increases. The same qualitative behavior also is exhibited by the (−)-TB enantiomer. Thus, we can conclude that in this case the IAS model predicts that, in the region of low concentration of each enantiomer, its adsorption is favored by increasing the concentration of the other enantiomer, while at high concentrations the usual competitive behavior is observed. This analysis, applied to literature data (Seidel-Morgenstern and Guiochon, 1993), leads to similar results where the synergistic effect is even stronger. This proves that the behavior exhibited by our system does not depend on the particular parameters used in the single-component isotherms, but is due to the peculiar shape of the (+)-TB isotherm. Finally, when the integrals Eq. 4 are explicit, it is possible to obtain an explicit solution that accounts for the effect of the concentration on the Henry constants without solving the nonlinear system of Eqs. 3 to 5. Therefore, in these cases the existence of this unusual behavior can be checked straightforwardly.

It is worth noting that, when using single-component Langmuir models, this kind of behavior is not observed. Similarly, it is not observed when using the RAS model, as shown in Figure 3 for the TB-(+) enantiomer. It is then to be concluded that this kind of adsorption synergies, which is pre-

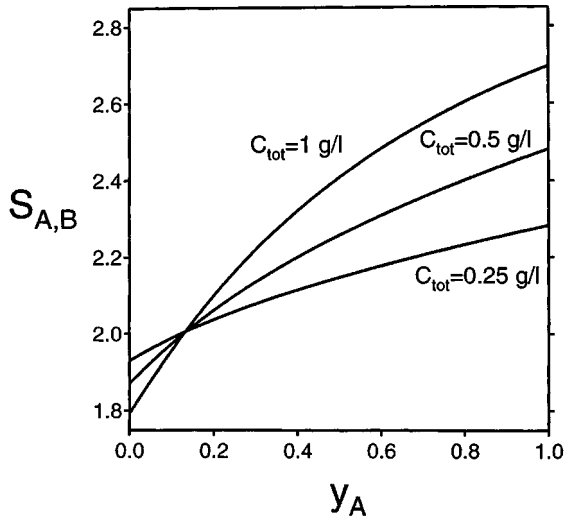

Figure 1. Selectivity $S_{A,B}$ calculated with the RAS model as a function of the composition in the liquid phase at different total concentrations.

By comparing points A–F, J–O, B–H, and K–P in Table 1 (where, due to experimental error, the total concentration is constant within 5%), it is possible to see that the selectivity is experimentally increasing with the molar fraction of the more retained species. As the total concentration decreases, the selectivity decrease is more pronounced.

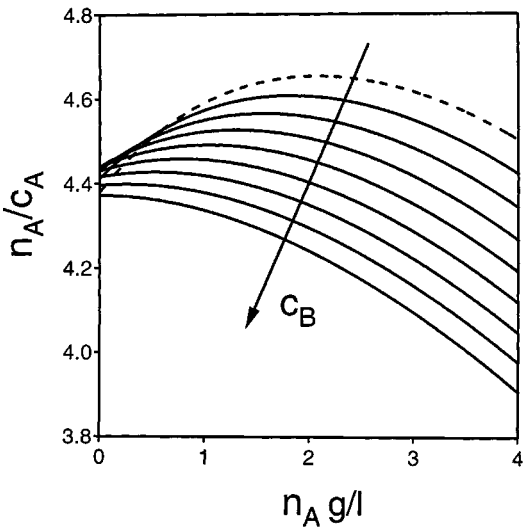

Figure 2. n/c vs. n plot of the (+)-TB enantiomer calculated with the IAS model.

Parametric curves at different concentrations of the less retained enantiomer. Starting from the top right corner of the figure $c_B = 0$ (broken line), 0.2, 0.4, 0.6, 0.8, 1, 1.2, 1.4, 1.6 g/L.

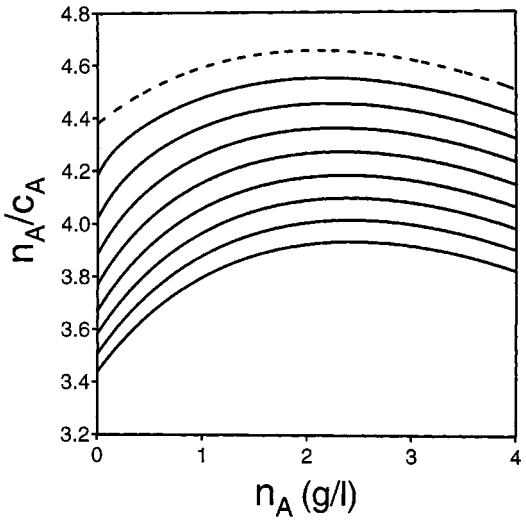

Figure 3. n/c vs. n plot of the (+)-TB enantiomer calculated with the RAS model.

Parametric curves at different concentrations of the less retained enantiomer as in Figure 2.

dicted by the IAS model at low concentrations, is not confirmed by the experimental evidence. This is probably an artifact of the IAS model related to the use of the single-component quadratic isotherm. Nevertheless, this could have negative consequences in unit design, leading to an exceedingly optimistic prediction of the equilibrium adsorbed amounts. Finally, the IAS model does not predict the existence of a maximum when the concentration of the (−)-TB enantiomer is high enough; this also implies that the inflection point in the multicomponent isotherm of (+)-TB enantiomer disappears. On the other hand, the RAS predicts the existence of a maximum in the whole range of concentrations studied, as shown in Figure 3.

Column Dynamics

Mathematical model

The simplest model of a chromatographic column that accounts for finite column efficiency is the equilibrium dispersive model, where the contribution of band broadening due to finite mass-transfer limitation and axial dispersion are lumped into an apparent axial dispersion coefficient. This model has been used to describe the chromatographic separation of the Tröger's base enantiomers on CTA, but using an apparent axial dispersion coefficient for the (+)-TB enantiomer that is 1.6 times larger than for the (−)-TB enantiomer (Seidel-Morgenstern and Guiochon, 1993), since it is known that the column efficiency (in terms of the number of theoretical plates) is different for the two enantiomers of the Tröger's base (Rizzi, 1989a,b). As reported in the literature, for operating conditions close to those adopted in this work, the column efficiency is controlled by eddy diffusion and mass-transfer resistance (Rizzi, 1989a; Jacobson et al., 1993). The latter provides the largest contribution to HETP (Rizzi, 1989a; Seidel-Morgenstern et al., 1993), whereas the former is the same for both enantiomers (Jacobson et al., 1993). This is because fluid mechanics phenomena do not distinguish between the two enantiomers, which, on the other hand, interact differently during transport through the particle and adsorption/desorption with the chiral stationary phase.

Therefore, it is more covenient to use a model where the effect of finite mass transfer and axial dispersion are decoupled, such as in the solid film linear driving force model ($i = A, B$):

$$\epsilon\frac{\partial c_i}{\partial t} + (1-\epsilon)\frac{\partial n_i}{\partial t} + u\frac{\partial c_i}{\partial x} = \epsilon D\frac{\partial^2 c_i}{\partial x^2} \tag{10}$$

$$\frac{\partial n_i}{\partial t} = k_i a_p (n_i^{eq} - n_i), \tag{11}$$

where n_i^{eq} is the adsorbed phase concentration in equilibrium with the fluid phase of composition c, and it is calculated using either the IAS or the RAS model (see the Notation section for all symbols not already defined in the text). According to the earlier discussion the same axial dispersion coefficient for the two enantiomers is used. In particular, this has been estimated from the Chung and Wen relationship as equal to 5×10^{-4} cm^2/s and kept constant in all the simulations.

Finally, the mass-transfer coefficients have been estimated through a simple one-parameter fitting of the frontal-analysis steps measured for determining the single-component isotherms. Though in the literature it is reported that these coefficients are composition dependent (Rearden et al., 1998), we have found that, at least within the concentration range considered in this work, they can be kept constant in order to describe, within the accuracy of the experimental error, the breakthrough profiles. Therefore, in the simulations the constant values $k_A a_p = 0.09$ s^{-1} and $k_B a_p = 0.15$ s^{-1} have been used, corresponding to the numbers of theoretical plates $N_{A,p}^{sol} = 68$ and $N_{B,p}^{sol} = 88$ at the superficial velocity of $u = 0.05$ cm/s. It is worth noting that the efficiency difference between the two enantiomers is small and that the more retained enantiomer has a lower number of theoretical plates. This is consistent with previous results, which show that at the linear velocity considered in this work the difference between the number of plates of the two enantiomers is small, while it increases significantly at higher flow rates (Rizzi, 1989a; Jacobson et al., 1993; Seidel-Morgenstern and Guiochon, 1993).

Adsorption/desorption experiments

In this section the adsorption/desorption experiments at different concentrations and relative composition reported in Table 1 are discussed and compared with the results of the numerical simulations. The IAS and RAS models are used together with the parameters determined in the previous section; thus the mathematical model is used in a purely predictive way with no fitting on the breakthrough data points. The on-line detection scheme used in this work allows the tracking of the absolute concentration of each enantiomer independently; the price to pay is a rather complex experimental setup that requires a fine calibration of the two detectors. However, the obtained information allows a thorough analysis of the adsorption behavior of the system.

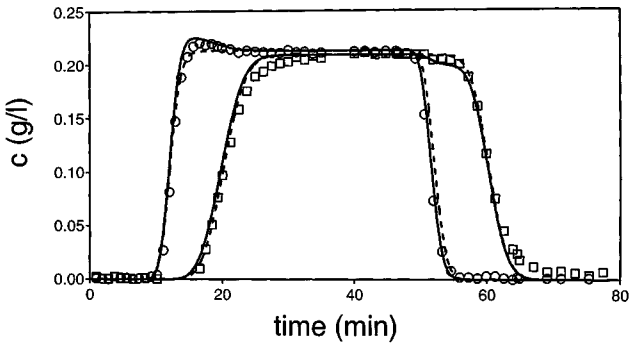

Figure 4. Experimental and calculated profiles for the adsorption/desorption step at the feed concentration of $c_A = 0.209$ g/L and $c_B = 0.213$ g/L (run F in Table 1).

The relative composition is 50/50. Symbols: ○ (−)-TB; □ (+)-TB. The solid lines are the profiles calculated with the RAS model, while the broken lines are calculated with the IAS model.

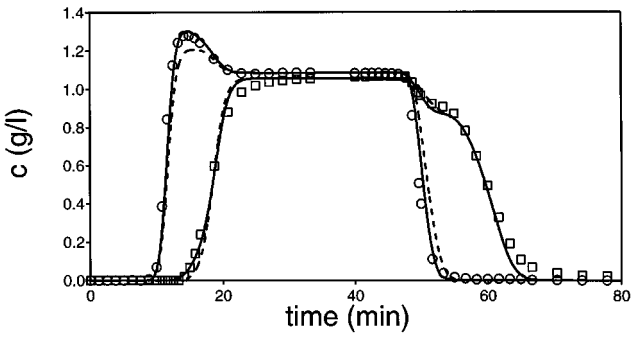

Figure 6. Experimental and calculated profiles for the adsorption/desorption step at the feed concentration of $c_A = 1.067$ g/L and $c_B = 1.095$ g/L (run K in Table 1).

The relative composition is 50/50. See Figure 4 for symbols.

First let us consider experiments where a one-to-one feed mixture of the two enantiomers diluted in ethanol is used, that is, runs E to L in Table 1. In all these and the following runs, the duration of the adsorption and desorption steps is 40 and 250 min, respectively (of which only 40 + 40 min is shown in Figures 4 to 6). The experimental results and calculated profiles for runs F, I, and K in Table 1 are shown in Figures 4, 5, and 6, where the symbols represent the experimental data as obtained through on-line analysis, whereas solid and broken lines are model predictions using the RAS and IAS model, respectively.

In the adsorption step the less retained enantiomer is eluted through the first transition, and its concentration reaches a plateau corresponding to an intermediate state where only (−)-TB is detected. Then the concentration of (−)-TB levels out, while (+)-TB breaks through, and both reach the feed concentration value. It is worth noting that the feed compositions are not racemic, because the solutions were prepared from the pure enantiomers. As already mentioned, from the areas underneath the breakthrough profiles it is possible to calculate the amount of each of the two enantiomers adsorbed. In Figures 4, 5, and 6 it is seen that the areas calculated for the (−)-TB enantiomer using the IAS model are smaller than the ones obtained experimentally. This is consistent with the data reported in Table 1, which show that the IAS model overestimates the amount of (−)-TB adsorbed by 5.5%, 10.1%, and 14.0% in runs F, I, and K. The RAS model underestimates the amount of (−)-TB adsorbed at low concentrations and overestimates it at high concentrations, the error always being within 4%. The roll-up of (−)-TB in the intermediate state is the result of the displacement of the less retained species by the strongly retained (+)-TB, and it is due to the competition of the enantiomers in adsorption under the overload nonlinear conditions of the experiments. At a low feed concentration (Figure 4) the IAS model does not predict any significant competition, while the RAS model and the experimental points already show a slight roll-up effect. As the feed concentration increases (Figures 5 and 6), that is, the adsorption is more and more nonlinear, the roll-up is stronger. This is not only due to the increasing nonlinearity of the adsorption equilibrium but also to an increase in the selectivity, as shown in Figure 7. It is rather evident from these results that the IAS model fails to account correctly for the competition of the two enantiomers and underestimates the concentration of the (−)-TB-rich intermediate state. On the other hand, the RAS model shows a reasonable accuracy in the whole range of concentrations.

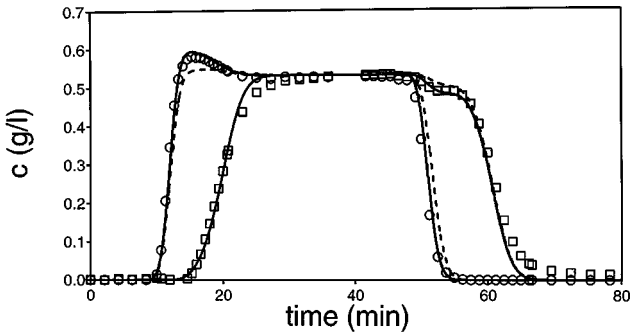

Figure 5. Experimental and calculated profiles for the adsorption/desorption step at the feed concentration of $c_A = 0.531$ g/L and $c_B = 0.532$ g/L (run I in Table 1).

The relative composition is 50/50. See Figure 4 for symbols.

It is worth noticing that the breakthrough of the more retained enantiomer is sluggish at high concentration, showing a tail in the achievement of the feed concentration in Figures 4 to 6, as well as in the other experiments reported in Table 1 but not shown here. Both the RAS and IAS models fail to predict this tail. The same behavior has been previously reported (Seidel-Morgenstern et al., 1993; Rearden et al., 1998) and it cannot be explained on the basis of our results.

In the desorption step the less retained enantiomer is eluted first, while the more retained enantiomer achieves a plateau at a lower concentration than in the feed state, corresponding to an intermediate state where only (+)-TB is detected. Both the IAS and RAS models are able to predict the plateau composition in the desorption step with reasonable accuracy. The area of the breakthrough curve of (−)-TB in

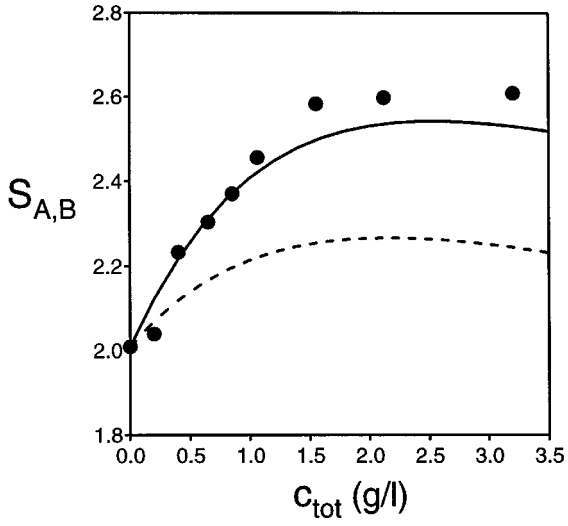

Figure 7. Selectivity at increasing total concentration at the racemic composition.

Symbols: ● experimental values. Solid line: RAS model; broken line: IAS model.

the desorption step, which was started at $t = 40$ min, is proportional to the amount of (−)-TB adsorbed, and it is overestimated by the IAS model. This is readily seen by noticing that the broken curve is shifted rightward with respect to the experimental points. Thus, summarizing, the calculations based on the IAS model show a weaker competition than the experimental results; this results in a lower intermediate plateau in the adsorption step and a larger amount of (−)-TB adsorbed, thus leading to a shift of the (−)-TB profiles in the desorption step.

Finally, the more retained enantiomer is eluted through the last transition and the column is regenerated. The desorption experiment always exhibits a long tail for the (+)-TB enantiomer. As for the tail in the adsorption step, the two models are not able to predict this behavior. The last transition deserves a further comment. Since the isotherm of the more retained enantiomer shows an inflection point at the concentration of 0.28 g/L, the nature of this transition changes in the different experiments. The concentration that discriminates between the two behaviors is about 0.5 g/L. In fact, at this point the slope of the tangent of the single-component isotherm (Eq. 2) and the chord connecting this point to the origin, are identical (Rhee et al., 1986). In Figure 4 the last transition where (+)-TB is elutes is a shock, because the (+)-TB enantiomer shows an unfavorable behavior at concentrations smaller than the inflection point. On the other hand, in Figure 6 the (+)-TB plateau has a concentration of about 0.9 g/L, and therefore a combined wave, that is, a wave at high concentration and a shock at low concentration, is expected (Rhee et al., 1986). This remark clarifies why the last transition is more spread in the run at higher concentrations, as appears evident by comparing Figures 4 and 6.

This study is completed by considering the experiments at different relative compositions in Table 1, that is, runs A to D and M to Q. The same remarks made before can be extended to the experiments illustrated in Figures 8 and 9, which refer to runs C and O, respectively. Moreover, it can be ob-

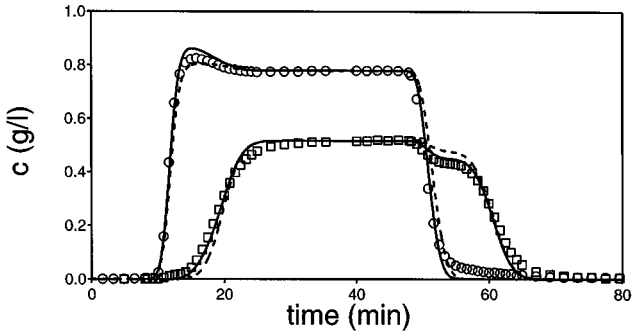

Figure 8. Experimental and calculated profiles for the adsorption/desorption step at the feed concentration of $c_A = 0.516$ g/L and $c_B = 0.779$ g/L (run C in Table 1).

The relative composition is 40/60. See Figure 4 for symbols.

served that increasing the relative amount of (+)-TB from 40% to 60% yields less competition, and hence a less pronounced roll-up in the (−)-TB breakthrough profile in Figure 8 than in Figure 9. Accordingly, the IAS model predicts well the experimental behavior in the case of run C, but fails to describe the (−)-TB profile in run O, thus confirming its difficulty in properly accounting for adsorption competition. This is consistent with all data in Table 1, where IAS performs well for both enantiomers at low (+)-TB relative concentrations (runs A to D), but performs poorly for the (−)-TB enantiomer at high (+)-TB relative concentration (runs M to Q). On the contrary, with a few exceptions, the RAS model is satisfactory at all compositions, such as, for example, run D. It is remarkably accurate in describing the roll-up profile in Figure 9. Furthermore, the RAS model also is more effective in predicting the desorption behavior, apart from the already mentioned tail of the more retained enantiomer. Differences between the experimental data and the IAS model results are observed in Figures 8 and 9 in the elution of the (−)-TB enantiomer and in the intermediate desorption plateau concentration of the (+)-TB enantiomer.

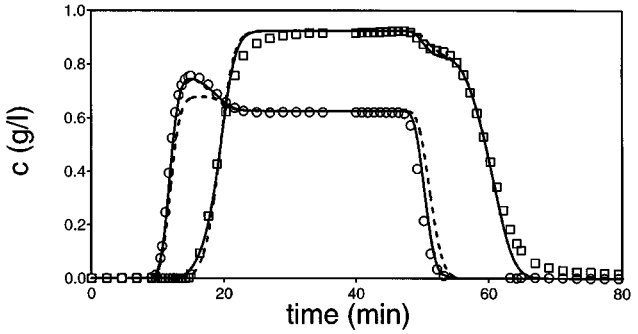

Figure 9. Experimental and calculated profiles for the adsorption/desorption step at the feed concentration of $c_A = 0.923$ g/L and $c_B = 0.626$ g/L (run O in Table 1).

The relative composition is 60/40. See Figure 4 for symbols.

It is worth noting that the accuracy in predicting the breakthrough and elution times is remarkably good for both the IAS and RAS models in all runs. This is a rather important feature from the practical point of view, where these models have to be used for the design of complex units such as simulated moving-bed units. In fact, in this case, breakthrough and elution times play a key role in defining optimal operating conditions; based on the preceding results it seems to be possible to use the simpler IAS model rather than the RAS model for this purpose.

Pulse experiments

The chromatograms of the racemic mixture and the pure enantiomers of this model system have been studied before in the literature. In particular, the chromatograms of the pure enantiomers show an unusual behavior, which has been investigated and explained (Seidel-Morgenstern and Guiochon, 1993). When increasing amounts of (−)-TB are injected, the retention time decreases, since this component adsorbs favorably. However, when this series of experiments is repeated with the (+)-TB enantiomer, first the retention time increases, and then, when larger amounts are injected, it starts to decrease (see Seidel-Morgenstern and Guiochon, 1993, figures 8 and 9). This unusual behavior is due to the nature of the adsorption of (+)-TB (unfavorable at low concentration and favorable at high concentration), and it is properly accounted for by the quadratic isotherm (Eq. 2). In this section the column model developed in the "Mathematical Model" and applied in the "Adsorption/Desorption Experiments" section, is used to simulate pulse chromatograms under nonlinear conditions. In Figure 10 the elution profile for the injection of 0.5 cm^3 of a racemic solution at a concentration of 3 g/L for each enantiomer, is reported. The results of the numerical simulations with the two thermodynamic models are almost the same, the only exception being the higher

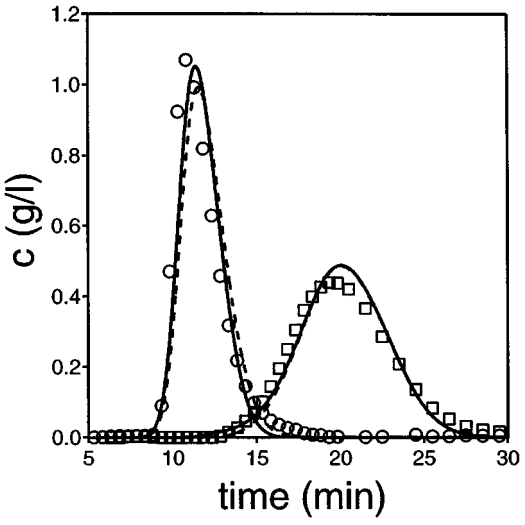

Figure 10. Experimental and calculated elution profiles for the injection of a sample of 0.5 cm^3 of a racemic solution at 3 g/L of each enantiomer: see Figure 4 for symbols.

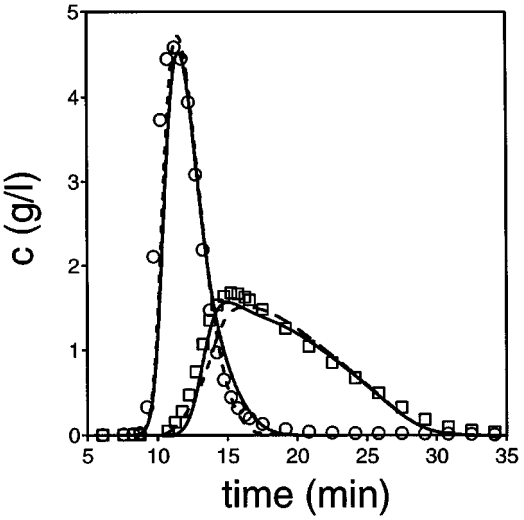

Figure 11. Experimental and calculated elution profiles for the injection of a sample of 2.5 cm^3 of a racemic solution at 3 g/L of each enantiomer: see Figure 4 for symbols.

peak of (−)-TB predicted by the RAS model. This is again due to the fact that the IAS model underestimates the competition between the two enantiomers, which agrees with previous observations in the literature (see Seidel-Morgenstern and Guiochon, 1993, figures 12 and 13). The results in Figure 10 confirm that the RAS model improves the description with respect to the IAS model, even though the tails shown by the experimental data are not well interpreted, as observed earlier in the adsorption/desorption experiments.

A second pulse experiment with an injected volume of 2.5 cm^3 is illustrated in Figure 11. Both models are in good qualitative agreement with the experimental results, which is remarkable since the concentration of the (−)-TB peak is more than two times higher than the largest concentration in the binary data of Table 1. Moreover, the single-component isotherms have been measured up to a concentration of about 2 g/L (Pedeferri et al., 1999). In this example the IAS model is able to predict the correct height of the (−)-TB peak, but the prediction of the retention time of the (+)-TB peak is wrong; however, the RAS model is in good agreement with both experimental peaks.

By comparing Figures 10 and 11 it can be seen that the increase in the volume injected leads to a decrease in the retention time of both enantiomers. It is interesting to run numerical pulse chromatography experiments at low concentrations to check whether the favorable/unfavorable behavior exhibited by the stronger enantiomer is retained in the binary experiments. In Figure 12 pulse chromatograms calculated at increasing volumes of racemic mixture are shown. These profiles are calculated with the RAS model, but the IAS model shows a similar pattern of behavior. The broken lines correspond to the breakthrough time of the two enantiomers, at infinite dilution. As the volume injected increases, the retention time of (−)-TB enantiomer becomes smaller, that is, the peak is shifted rightward. On the other hand, a slight increase in the retention time of the (+)-TB is observed, show-

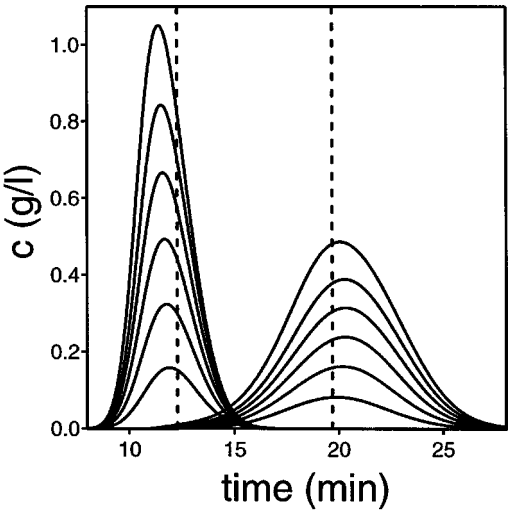

Figure 12. Elution profiles calculated with the RAS model for the injection of increasing samples of a racemic solution at 3 g/L of each enantiomer.

The volumes injected are 0.083, 0.166, 0.25, 0.33, 0.416, 0.5 cm^3. The broken lines are the breakthrough times calculated at infinite dilution.

ing a maximum corresponding to an injected volume of 0.25 cm^3. A further increase in the volume injected (compare Figure 10 and Figure 11) leads to a decrease in the retention time. Therefore the binary mixture is expected to exhibit the same qualitative behavior of the pure enantiomers, although the extent of the increase in the retention time is smaller.

Conclusions

The on-line monitoring scheme developed in this work provides a careful measurement of the individual breakthrough profiles of a racemic mixture. This allows the competitive adsorption behavior of the Tröger's base enantiomers on crystalline triacetylcellulose (CTA) to be studied in detail. The prediction of the binary competitive equilibrium given by the IAS model, which exploits only single-component isotherms, has been assessed and compared with that of the RAS model. The behavior of the IAS model, when applied to a quadratic isotherm, has been shown. In our case, and for other results in the literature, the model predicts an increase in the retention factor of one enantiomer at increasing concentrations of the other enantiomer.

The IAS model underestimates the extent of competition between the two enantiomers, and therefore the RAS model has been adopted. The activity coefficient of the RAS model depends on both composition and spreading pressure, which is in turn strongly dependent on composition. The two models have been assessed by calculating *a priori*, that is, by measuring all the needed dispersion parameters from single-component breakthrough curves, the nonlinear binary breakthroughs at different concentrations and compositions and the overload pulses. Both models predict well the breakthrough time of the different transitions even though only the RAS model describes quantitatively the entire concentration profiles. The proposed models can be used as a tool for the scale-up and optimization of batch and continuous chiral separations.

Notation

a_p = specific surface
A = adsorption surface
D = axial dispersion coefficient
k = overall mass-transfer coefficient
R = gas constant
t = time
T = temperature
x = column axial coordinate
y = mol fraction in the liquid phase
α = activity model parameter
Λ = activity model parameter
Π = spreading pressure

Subscripts and superscripts

i = component index, $i = A, B$
exp = experimental value
mod = model result
sol = solid-film linear driving-force model
tot = total concentration
$^\circ$ = pure component isotherm

Literature Cited

Costa, E., J. L. Sotelo, G. Calleya, and C. Marroń, "Adsorption of Binary and Ternary Hydrocarbon Gas Mixtures on Activated Carbon: Experimental Determination and Theoretical Prediction of the Ternary Equilibrium Data," *AIChE J.*, **27**, 5 (1981).

Fornstedt, T., P. Sjonz, and G. Guiochon, "Thermodynamic Study of an Unusual Chiral Separation: Propanol Enantiomers on an Immobilised Cellulase," *J. Amer. Chem. Soc.*, **119**, 1254 (1997).

Francotte, E., and J. Richert, "Application of Simulated Moving Bed Chromatography to the Separation of the Enantiomers of Chiral Drugs," *J. Chromatog. A*, **769**, 101 (1997).

Francotte, E., M. W. Romain, and D. Lohmann, "Chromatographic Resolution of Racemates on Chiral Stationary Phases. Influence of Supramolecular Structure of Cellulose Triacetate," *J. Chromatog.*, **347**, 25 (1985).

Gamba, G., R. Rota, S. Carrá, and M. Morbidelli, "Adsorption Equilibria of Nonideal Multicomponent Systems at Saturation," *AIChE J.*, **36**, 1736 (1990).

Gamba, G., R. Rota, R. Stori, S. Carrá, and M. Morbidelli, "Adsorbed Solution Theory Models for Multicomponent Adsorption equilibria," *AIChE J.*, **35**, 959 (1989).

Golshan-Shirazi, S., and G. Guiochon, "On the Use of the LeVan-Vermeulen Isotherm Model for the Calculation of Elution Band Profiles in Non-Linear Chromatography," *J. Chromatog.*, **545**, 1 (1991).

Heuer, C., E. Küsters, T. Plattner, and A. Seidel-Morgenstern, "Design of the Simulated Moving Bed Process Based on Adsorption Isotherm Measurements Using a Perturbation Method," *J. Chromatog. A*, **827**, 175 (1998).

Jacobson, S., S. Golshan-Shirazi, and G. Guiochon, "Chromatographic Band Profile and Band Separation of Enantiomers at High Concentration," *J. Amer. Chem. Soc.*, **112**, 6492 (1990).

Jacobson, S. C., S. Seidel-Morgenstern, and G. Guiochon, "Chromatographic Band Profile and Band Separation of Enantiomers at High Concetration," *J. Chromatog.*, **637**, 13 (1993).

Küsters, E., G. Gerber, and F. D. Antia, "Enantioseparation of a Chiral Epoxide by Simulated Moving Bed Chromatography Using Chiralcel-OD," *Chromatographia*, **40**, 387 (1995).

LeVan, M. D., and T. Vermeulen, "Binary Langmuir and Freundlich Isotherms for Ideal Adsorbed Solution," *J. Phys. Chem.*, **85**, 3247 (1981).

Migliorini, C., A. Gentilini, M. Mazzotti, and M. Morbidelli, ''Design of Simulated Moving Bed Units Under Non-Ideal Conditions,'' *Ind. Eng. Chem. Res.*, **38**, 2400 (1999).
Migliorini, C., M. Mazzotti, and M. Morbidelli, ''Modelling Simulated Moving Bed Units for the Separation of Fine Chemicals,'' *Fundamentals of Adsorption 98*, Elsevier, Amsterdam, p. 484 (1998).
Myers, A. L., ''Activity Coefficients of Mixtures Adsorbed on Heterogeneous Surfaces,'' *AIChE J.*, **29**, 691 (1983).
Myers, A. L., ''New Technique for Rapid Measurements of Equilibrium Adsorption from Binary Gas Mixtures,'' *Proc. World Cong. III of Chem. Eng.*, Tokyo, p. 902 (1986).
Myers, A. L., and J. M. Prausnitz, ''Thermodynamics of Mixed Gas Adsorption,'' *AIChE J.*, **11**, 121 (1965).
Nicoud, R. M., G. Fuchs, P. Adam, M. Bailly, E. Küsters, F. D. Antia, R. Reuille, and E. Schmid, ''Preparative Scale Enantioseparation of a Chiral Epoxide: Comparison of Liquid Chromatography and Simulated Moving Bed Adsorption Technology,'' *Chirality*, **5**, 267 (1993).
O'Brien, J., and A. L. Myers, ''Rapid Calculations of Multicomponent Adsorption Equilibria from Pure Isotherm Data,'' *Ind. Eng. Chem. Process Des. Dev.*, **24**, 1187 (1985).
Pais, L. S., J. M. Loureiro, and A. E. Rodrigues, ''Separation of 1-1′-bi-2-Naphtol Enantiomers by Continuous Chromatography in Simulated Moving Bed,'' *Chem. Eng. Sci.*, **52**, 245 (1997).
Paludetto, R., G. Storti, G. Gamba, S. Carrá, and M. Morbidelli, ''On Multicomponent Adsorption Equilibria of Xylene Mixtures on Zeolites,'' *Ind. Eng. Chem. Res.*, **26**, 2250 (1987).
Pedeferri, M., G. Zenoni, M. Mazzotti, and M. Morbidelli, ''Experimental Analysis of a Chiral Separation Through Simulated Moving Bed Chromatography,'' *Chem. Eng. Sci.*, **54**, 3735 (1999).
Radke, C. J., and J. M. Prausnitz, ''Thermodynamics of Multi-Solute Adsorption from Dilute Liquid Solutions,'' *AIChE J.*, **18**, 761 (1972).
Rearden, P., P. Sajonz, and G. Guiochon, ''Detailed Study of the Mass Transfer Kinetics of Tröger's Base on Cellulose Triacetate,'' *J. Chromatog. A*, **813**, 1 (1998).
Rhee, H.-K., R. Aris, and N. R. Amundson, *First Order Partial Differential Equations*, Vol. 1, Prentice Hall, Englewood Cliffs, NJ (1986).
Rizzi, A. M., ''Band Broadening in High-Performance Liquid Chromatographic Separations of Enantiomers with Swollen Microcrystalline Cellulose Triacetate Packings: I. Influence of Capacity Factor, Analyte Structure, Flow Velocity and Column Loading,'' *J. Chromatog.*, **478**, 71 (1989a).
Rizzi, A. M., ''Band Broadening in High-Performance Liquid Chromatographic Separations of Enantiomers with Swollen Microcrystalline Cellulose Triacetate Packings: II. Influence of Eluent Composition, Temperature and Pressure," *J. Chromatog.*, **478**, 87 (1989b).
Seidel-Morgenstern, A., and G. Guiochon, ''Modeling of the Competitive Isotherms and the Chromatographic Separation of Two Enantiomers,'' *Chem. Eng. Sci.*, **48**, 2787 (1993).
Seidel-Morgenstern, A., S. C. Jacobson, and G. Guiochon, ''Study of Band Broadening in Enantioselective Separations Using Microcrystalline Cellulose Triacetate: II. Frontal Analysis,'' *J. Chromatog. A*, **637**, 19 (1993).
Talu, O., and A. L. Myers, ''Rigorous Thermodynamic Treatment of Gas Adsorption,'' *AIChE J.*, **34**, 1887 (1988).
Talu, O., and I. Zwiebel, ''Multicomponent Adsorption Equilibria of Nonideal Mixtures,'' *AIChE J.*, **32**, 1263 (1986).
Valenzuela, D. P., A. L. Myers, O. Talu, and I. Zwiebel, ''Adsorption of Gas Mixtures: Effect of Energetic Heterogeneity,'' *AIChE J.*, **34**, 397 (1988).
Zenoni, G., M. P. Pedeferri, M. Mazzotti, and M. Morbidelli, ''On-Line Monitoring of Enantiomer Concentration in Chiral Simulated Moving Bed Chromatography,'' *J. Chromatog. A*, in press (2000).

Manuscript received Oct, 20, 1999, and revision received Mar. 2, 2000.